OPEN ACCESS

ACTA METALLURGICA SLOVACA

2026, VOL. 32, NO. 2, 102-109

SCICELL

RESEARCH PAPER

Calculation of activation energy at hot plastic deformation conditions

Rudolf Pernis[1], Michal Krbaťa[2], Daniel Pernis[3], Tibor Kvačkaj[4]*

[1] *Bodva Industry and Innovation Cluster, Budulov 174, 04501, Moldava n/B, Slovak Republic*
[2] *Alexander Dubcek University of Trencin in Trencin, Faculty of Special Technology, Ku kyselke 469, 911 06 Trenčín, Slovak Republic*
[3] *Masaryk University, Faculty of Informatics, Botanická 554/68a, 602 00 Brno, Czech Republic*

*Corresponding author: *e-mail: tibor.kvackaj@biic.sk@seznam.cz, Bodva Industry and Innovation Cluster, Department of RDI, Budulov 174, 04501, Moldava nB, Slovak Republic*

Received: 25.05.2025
Accepted: 08.06.2026

ABSTRACT

For experiments to determine heat-induced deformation resistance, boron-added steel, officially designated as BCT steel, was used. This designation characterizes steel that does not belong to the standardized steel brands. Deformation resistance was determined using a hardening dilatometer, DIL805A/D, supplemented with a hydraulic unit. This enables compression tests during high-temperature forming. The deformation mode allows the material to be formed under defined conditions. Such conditions are strain, temperature, and strain rate. The deformation resistance for the 5x5 test matrix, deformation temperatures (800, 900, 1000, 1100, 1200 °C), and deformation rates (0.001, 0.01, 0.1, 1, 10 s^{-1}) were experimentally determined. A mathematical model was used to evaluate the measured data, describing the deformation curve as a function of deformation. Furthermore, equations were used to calculate the basic deformation resistance as a function of two variables: the degree of deformation and the deformation temperature, with the deformation rate held constant. Appropriate mathematical equations and their graphical visualisation are given for the five deformation rates. The Garofalo equation is used to calculate the activation energy of plastic deformation under heat. This equation is further extended by the deformation variable. Based on the results of the physical simulation of the compression process, a mathematical model was developed. From the deformation curves, obtained through mathematical simulation of the compression process, it was possible to calculate the activation energy of plastic deformation at different temperatures. Subsequent visualisation of the activation energy values showed their dependence on the deformation temperature. The mathematical description showed that the activation energy of plastic deformation depends on the deformation temperature, indicating that it is not a constant value as has been reported so far.

Keywords: *Garofalo equation; Boron steel*; *numerical solution; hot compression test; deformation curve; strain resistance function; activation energy*

INTRODUCTION

The semi-empirical Garofalo equation is used to describe high-temperature deformation, which expresses the deformation stress as a function of strain rate and absolute deformation temperature

$$\dot{\varphi} \cdot exp\left(\frac{Q}{RT}\right) = C\left[sinh(\alpha \cdot \sigma_p)\right]^n \quad (1)$$

where: $\dot{\varphi}$ [s^{-1}] – strain rate,
T [K] – absolute temperature,
σ_p [MPa] – peak stress (flow stress),
Q [$J.mol^{-1}$] – activation energy of deformation,
R [$J.K^{-1}.mol^{-1}$] – universal gas constant,
n [–] – material constant,
C [s^{-1}] – material constant,
α [MPa^{-1}] – material constant.

Eq. (1) is rewritten in the literature [3–5] into the form

$$\dot{\varphi} = C \cdot exp\left(-\frac{Q}{RT}\right)\left[sinh(\alpha \cdot \sigma_p)\right]^n \quad (2)$$

Determination of the material constant α. According to [6–8], the determination of the material constant α is based on the following consideration. For high deformation temperatures and low deformation rates, the condition applies $\sigma_p < 1$, which allows Eq. (2) to be reduced to the form

$$\dot{\varphi} = C' \cdot exp\left(-\frac{Q}{RT}\right)\sigma_p^{n_1} \quad (3)$$

Constant n_1 represents a material constant. For the condition $\sigma_p > 1$, which represents forming occurring at lower temperatures and higher deformation rates, Eq. (2) can be reduced to the form

$$\dot{\varphi} = C'' \cdot exp\left(-\frac{Q}{RT}\right) exp(\beta \cdot \sigma_p) \quad (4)$$

where: $\alpha = \frac{\beta}{n_1}$ (5)

$\beta = const.$ (6)

and β is a material constant. For the calculation of the constant n_1 in Eq. (3), the values of the peak stress of the curve at the highest deformation temperature are used. For the calculation of the material constant β in Eq. (4), the values of the peak stress of the curve at the lowest deformation temperature are used.

Determination of material constants n, Q, and C. The original methodology for calculating material constants, proposed by Garofalo, was published in [9]. This methodology is based on the principle of linear dependence between two variables, with the other variable treated as a constant. A simple linear regression was used for the calculation itself. For example, the material constant *n* is calculated separately for each deformation temperature. Their average value is considered the resulting material constant *n* for Eq. (2). The activation energy *Q* is determined similarly. The calculated values of material constants *n*, *Q*, and *C* are subject to certain errors. Knowing the material constant α, Pernis [10] proposed increasing the accuracy and simplifying the calculation method of the other material constants *n*, *Q*, and *C*. Multiple linear regression was used for the calculation. The Garofalo equation in the form of Eq. (1) describes the dependence of peak stress on strain rate and deformation temperature. Four material constants appear further in the equation. For extending the Garofalo equation by a functional dependence on deformation, the material

constants were replaced by polynomial functions. Polynomials of 5th degree [11, 12], 6th degree [13–15], and 8th degree [16] were used. In [17] a 9th degree polynomial with 40 constants was used. For the purpose of extending Eq. (1) by an additional variable, deformation, a functional dependence of the material constants on deformation was sought: $\alpha(\varphi)$, $n(\varphi)$, $Q(\varphi)$ a $C(\varphi)$. Garofalo's Eq. (1), extended by the variable deformation φ, was expressed as

$$\dot{\varphi} \cdot exp\left(\frac{Q(\varphi)}{RT}\right) = C(\varphi)[sinh(\alpha(\varphi) \cdot \sigma)]^{n(\varphi)} \quad (7)$$

where the individual deformation functions were sought in the form of

$$\alpha(\varphi) = A_0 + A_1\varphi + A_2\varphi^2 + A_3\varphi^3 + A_4\varphi^4 + A_5\varphi^5 \quad (8)$$

$$n(\varphi) = n_0 + n_1\varphi + n_2\varphi^2 + n_3\varphi^3 + n_4\varphi^4 + n_5\varphi^5 \quad (9)$$

$$Q(\varphi) = Q_0 + Q_1\varphi + Q_2\varphi^2 + Q_3\varphi^3 + Q_4\varphi^4 + Q_5\varphi^5 \quad (10)$$

$$ln\ C(\varphi) = C_0 + C_1\varphi + C_2\varphi^2 + C_3\varphi^3 + C_4\varphi^4 + C_5\varphi^5 \quad (11)$$

Based on a literature review, it was found that the temperature dependence of the activation energy of hot plastic deformation has not yet been described. The activation energy over the entire range of deformation and deformation temperature was considered constant.

Mathematical model of deformation curves. For this purpose, a mathematical model proposed by Pernis and Škrobian [18] is used. The equation of deformation stress, which would describe the deformation curve as a function of deformation at constant strain rate and constant deformation temperature, is based on a one-dimensional mathematical model [18]:

$$\sigma = \sigma_0 \varphi^{a_0} e^{F(\varphi)}\Big|_{\dot{\varphi}=const,\ t=const} \quad (12)$$

where: σ [MPa] – flow stress (deformation resistance),
σ_0 [MPa] – material constant,
a_0 [–] – material constant,
$F(\varphi)$ [–] – suitably chosen deformation function,
t [°C] – temperature deformation
φ [–] – logarithmic deformation.

The function $F(\varphi)$ used in Eq. (12) allows the mathematical model to be defined as an open model, which can be adapted to the needs of describing measured data. The solution was found in the use of simple rational functions:

$$F(\varphi) = b_1\varphi^{-2} + b_2\varphi^{-1} + b_3\varphi + b_4\varphi^2 + b_5\varphi^3 \quad (13)$$

where b_1 to b_5 are dimensionless constants. The calculation of the constants in Eq. (12) was carried out using general linear regression. This allowed for the logarithmization of Eq. (12):

$$ln\,\sigma = ln\,\sigma_0 + a_0\,ln\,\varphi + b_1\varphi^{-2} + b_2\varphi^{-1} + b_3\varphi + b_4\varphi^2 + b_5\varphi^3 \quad (14)$$

In further study, Eq. (12) was expanded to two independent variables. Deformation resistance depending on deformation and deformation temperature at a constant strain rate. Eq. (12) was extended by the variable deformation temperature t. The constant a_0 was replaced by a suitably chosen temperature function $E(t)$, and the F–function was supplemented by deformation temperature. Eq. (12) then took the new form [18]

$$\sigma = \sigma_0 \varphi^{E(t)} e^{F(\varphi,t)}\Big|_{\dot{\varphi}=const} \quad (15)$$

where: σ [MPa] – flow stress (deformation resistance),
t [°C] – deformation temperature,
$E(t)$ [–] – suitably chosen function of the deformation temperature,
$F(\varphi, t)$ [–] – suitably chosen function of deformation and temperature.

The following equation proved suitable as the E–function:

$$E(t) = a_0 + a_1 t + a_2 t^2 + a_3 t^3 \quad (16)$$

Constants a_0 to a_3 have dimensions chosen to compensate the dimension of temperature to a dimensionless value. In some cases, it proved useful to transform the deformation temperature t to a transformed value $ln(t)$ or $t/1000$. The F–function was supplemented by the deformation temperature variable:

$$F(\varphi,t) = b_1\varphi^{-3} + b_2\varphi^{-2} + b_3\varphi^{-1} + b_4\varphi + b_5\varphi^2 + b_6\varphi^3 + b_7 t + b_8 t^2 + b_9 t^3 + (b_{10}\varphi^{-3} + b_{11}\varphi^{-2} + b_{12}\varphi^{-1} + b_{13}\varphi + b_{14}\varphi^2 + b_{15}\varphi^3)t^{-1} \quad (17)$$

Constants b_1 to b_{15} have dimensions chosen to compensate the dimension of temperature to a dimensionless value.

EXPERIMENTAL MATERIAL AND METHODS

For the experiments, steel with a boron addition, designated as BCT steel, was used. This designation characterizes steel that does not belong to normalized steel grades. The chemical composition of the steel is provided in **Table 1**.

Practical compression tests to measure deformation resistance were carried out using the Dilatometer DIL805A/D device. The test specimen geometrically consisted of a cylinder with a diameter $D=5$ mm and a length $L=10$ mm. Sample heating was ensured by electric induction heating. For measuring deformation resistance, the temperatures chosen were 800, 900, 1000, 1100, and 1200 °C. Logarithmic strain was continuously measured in the range from 0 to 0.9. Specific strain rates of 0.001, 0.01, 0.1, 1, and 10 s^{-1} were selected for deformation resistance measurement. From the viewpoint of deformation temperature and strain rate, a full experimental 5x5 matrix was studied. For numerical modeling of the compression test process, a mathematical model of deformation curves was developed. Through numerical modeling, deformation curves for additional deformation temperatures were obtained, enabling the calculation of activation energy. The result of numerical modeling was determining the activation energy for narrowed temperature intervals of deformation. The obtained activation energy values allowed examining the values of activation energy depending on deformation temperature.

Table 1 Chemical composition of BCT steel (mass %)

Element	**C**	**Mn**	**Si**	**P**	**Cr**	**V**	**Mo**
Composition	0.12	1.60	0.45	0.013	0.04	0.002	0.02
Element	**Ni**	**Nb**	**Al**	**S**	**W**	**B**	**Fe**
Composition	0.07	0.04	0.03	0.005	0.01	0.002	balance

RESULTS AND DISCUSSION

Through compression tests, 25 deformation curves were obtained, shown in **Fig. 1**. **Fig. 2** presents a visualization of the measured peak stress σ_p as a function of strain rate, with deformation temperature as the parameter for each curve. The peak stress represents the maximum stress value on the respective deformation

Table 2 Material constant n

i	**t_i (°C)**	**n_i (-)**	**R^2_i**
1	800	4.6842	0.9623
2	900	4.4877	0.9729
3	1000	4.8644	0.9864
4	1100	5.1984	0.9814
5	1200	4.8318	0.9962
Sum	-	24.0665	-
Average	-	**4.8133**	-

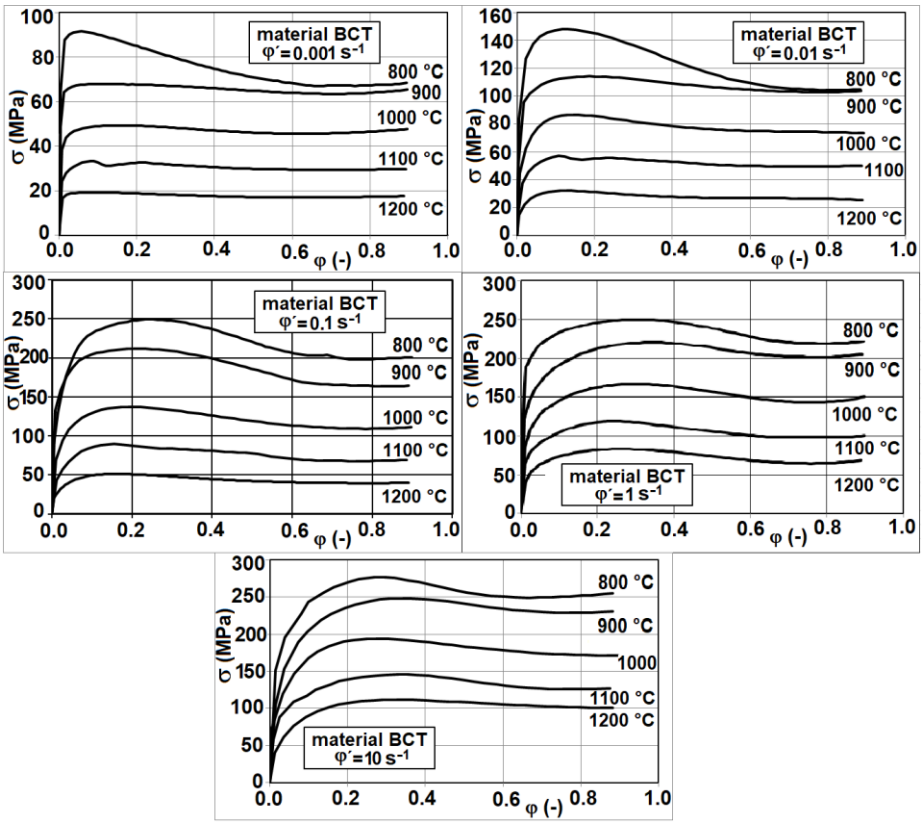

Fig. 1 True Strain –True Stress curves for BCT steel

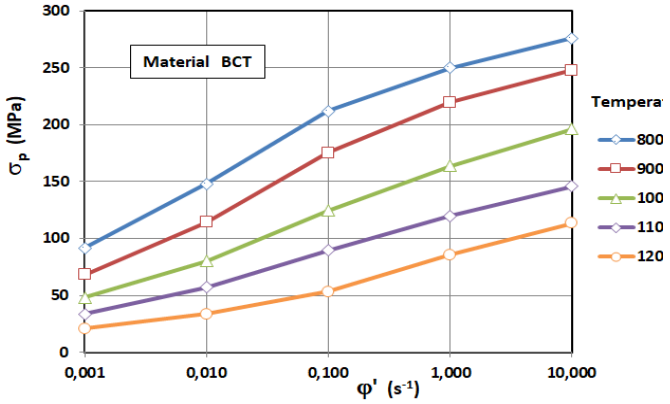

Fig. 2 Dependence of peak stress on strain rate

curve (see **Fig. 1**). From the 25 deformation curves, 25 peak stress values were determined. The Garofalo Eq. (1) was applied to peak stress. For the calculation of the constant n_1 in Eq. (3), peak stress values from the curve at 1200 °C on **Fig. 2** were used. The material constant has a value of n_1=5.264149. For the calculation of the material constant β in Eq. (4), peak stress values from the curve at 800 °C on **Fig. 2** were used. The material constant β has a value of β=0.047557 MPa^{-1}. The material constant α for the Garofalo Eq. (1), determined from Eq. (5), has a value of α=0.009034 MPa^{-1}. For the calculation of the material constant n for peak stress using the Garofalo method, see **Table 2** (n=4.8133). Similarly, the calculation of activation energy Q for peak stress is documented in **Table 3** (Q=270.858 kJ.mol^{-1}).

Table 3 Activation energy Q

i	φ' (s^{-1})	Q_i (kJ.mol^{-1})	R^2_i
1	0.001	247.116	0.9754
2	0.01	270.119	0.9749
3	0.1	296.383	0.9728
4	1	277.797	0.9757
5	10	262.872	0.9730
Sum	-	1354.2877	-
Average	-	**270.858**	-

Table 4 Comparison of calculation constants according to Garofalo and Pernis methodology

Constant	Unit	Garofalo [9]	Pernis [10]	Difference
α	MPa^{-1}	0.009034	0.009034	0
n	–	4.813300	4.902056	-0.088756
Q	kJ.mol^{-1}	270.857541	275.85208	-4.994538
$ln\ C$	ln s^{-1}	23.134883	23.112664	+0.022219
Sum Sqr	MPa^2	5628.133	**3794.973**	+1833.160

Comparison of the results of calculating material constants for peak stress according to the methodologies of Garofalo [9] and Pernis [10] is shown in **Table 4**. The accuracy evaluation of the deformation peak stress calculation was conducted using the sum of squares of the difference between measured and calculated stress, $\Sigma(\sigma_{meas}-\sigma_{calc})^2$. The calculation of material constants according to Pernis's methodology shows a significantly lower sum of squares, indicating that the material constants were determined with higher precision.

Material constants α, n, Q and C as functions of deformation. From the deformation curves shown in **Fig. 1**, the corresponding deformation stress values were first determined for deformation φ=0.1 to 0.8 with a constant step $\Delta\varphi$=0.05. A total of 15 data sets were obtained, each set containing 25 deformation stress values. The material constants $\alpha(\varphi)$, $n(\varphi)$, $Q(\varphi)$ and $C(\varphi)$ were determined separately for each data set from Garofalo's Eq. (18):

$$\dot{\varphi} \cdot exp\left(\frac{Q(\varphi)}{RT}\right) = C(\varphi)[sinh(\alpha(\varphi) \cdot \sigma)]^{n(\varphi)}\Big|_{\varphi'=const} \quad (18)$$

From the calculated 15 quadruples of material constants, the constants for Eq. (8) to Eq. (11) were determined. The calculated constants A_i, n_i, Q_i, and C_i (for i=0 to 5) are listed in **Table 5**. The activation energy Q_i was determined using the calculation methodology according to Pernis [10]. The paired coordinate points of the constants and deformation α–φ, n–φ, Q–φ and $ln(C)$–φ are visualized in graphs in **Fig. 3**. For comparison of calculated activation energy values according to the methodologies of Garofalo [9] and Pernis [10], a graph was produced, shown in **Fig. 4**. From the given graph, it follows that the activation energy values calculated by Pernis's methodology are approximately 100 kJ·mol^{-1} higher than those calculated by Garofalo's methodology. The calculated values of deformation resistance as a function of deformation were carried out from the equation:

$$\sigma = \frac{1}{\alpha(\varphi)} argsinh\left(\left(\frac{\dot{\varphi}}{C(\varphi)} e^{\frac{Q(\varphi)}{RT}}\right)^{1/n(\varphi)}\right) \quad (19)$$

The visualization of the comparison between measured and calculated values of deformation resistance is shown in **Fig. 5**. The graph is prepared for a constant deformation rate φ'=0.1 s^{-1}. The black curves represent the measured values of deformation stress, and the purple curves represent the calculated values from the mathematical model, Eq. (19). The calculated and measured values of deformation resistance show a significant difference, as documented by the correlation coefficient (R^2=0.9030). For this reason, a new mathematical model of deformation curves was sought to more accurately describe the deformation curves.

Table 5 Material constants for Eq. (8) to (11)

i	A_i (MPa^{-1})	n_i (-)	Q_i (kJ.mol^{-1})	C_i (ln s^{-1})
0	0.009723	7.315676	437.738387	39.160611
1	0.001981	-22.311054	-1590.550978	-160.250969
2	-0.049054	72.344513	5949.512220	613.771766
3	0.172226	-116.374882	-11467.052987	-1192.299514
4	-0.214534	95.405015	11229.646740	1167.051242
5	0.089835	-31.880095	-4375.469961	-452.658465
R^2	0.9946	0.9984	0.9977	0.9985

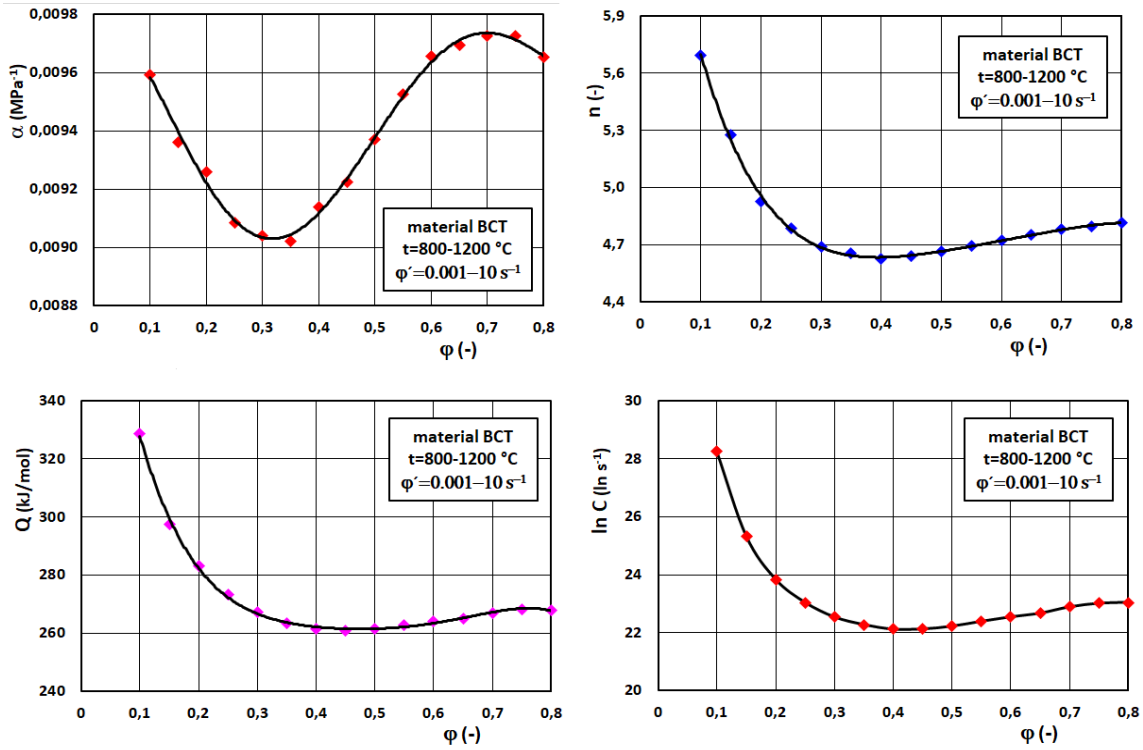

Fig. 3 Dependence of material constants α, n, Q end $ln\ C$ on deformation

The mathematical model of deformation curves. For this purpose, the mathematical model proposed by Pernis and Škrobian [18] was used. To describe a single deformation curve, a one-dimensional mathematical model given by Eq. (12) and a function $F(\varphi)$ specified by Eq. (13) is applied. An example of calculated coefficients for the deformation curve is shown in **Table 6**. The high value of the correlation coefficient (R^2=0.9981) confirms that the function $F(\varphi)$ in Eq. (13) is suitable for approximating deformation curves. The visualization of the measured and calculated deformation resistance under deformation conditions of t=800 °C and φ'=0.1 s^{-1} is shown in **Fig. 6**. For two independent variables, deformation and deformation temperature, the mathematical model given by Eq. (15) was used, with the function $E(t)$ given by Eq. (16) and the function $F(\varphi, t)$ given by Eq. (17). Eq. (15) to (17) were employed to visualize the measured and calculated values of BCT steel at temperatures of 800, 900, 1000, 1100, and 1200 °C at a constant deformation rate φ'=1 s^{-1}. The coefficients for Eq. (15) under the given deformation conditions are presented in **Table 7**. The resulting graph is

shown in **Fig. 7**. The black curves represent measured values of deformation resistance, while the red curves are calculated from the mathematical model Eq. (15). The value of the correlation coefficient (R^2=0.9990) indicates a very close fit of the mathematical model to the measured values. For the temperature of 950 °C, a forecast of the deformation curve (blue curve) was determined.

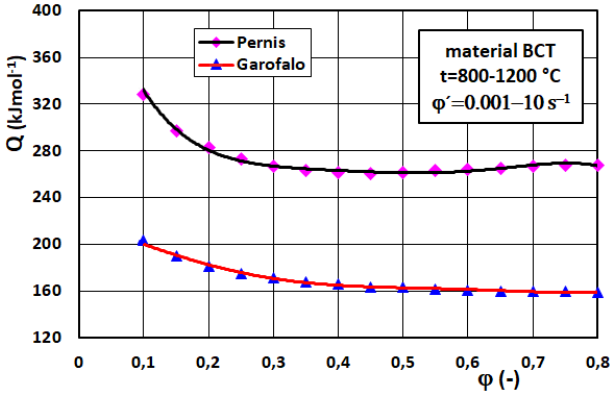

Fig. 4 Comparison of activation energy calculation results according to Garofalo and Pernis methodology

Table 6 Constants for the deformation curve in **Fig. 6**

Constant	Unit	Value
$ln\ \sigma_0$	*ln MPa*	5.702 496 668
a_0	–	0.154 509 157
b_1	–	-7.441 44E -09
b_2	–	-0.000 524 408
b_3	–	-0.048 040 299
b_4	–	-2.328 112 036
b_5	–	1.862 164 556
R^2	–	0.9981
t	°C	800
φ'	s^{-1}	0.1

The activation energy for hot plastic deformation. The activation energy for hot plastic deformation for the baseline set of measured peak stress data shown in **Fig. 2** has already been determined (see **Table 4**). This calculated activation energy is a constant value for the entire temperature range of forming, from 800 to 1200 °C. The dependence of activation energy on deformation is documented in the graph in **Fig. 3**. When activation energy is a function of deformation, it can be ***hypothesized*** that the activation energy is also a function of deformation temperature. If the procedure was analogous to finding the activation energy depending on the deformation value, additional measurements of deformation curves at other temperatures would be necessary. From the perspective of the measured deformation curves shown in **Fig. 1**, which were conducted with a step of Δt=100 °C, it would be necessary to refine the temperature step to Δt = (100/4) = 25 °C, ideally Δt = (100/4)/4 = (25/4) = 6.25 °C. The costs of conducting compression tests are relatively high and especially time-consuming. Therefore, mathematical-statistical methods were sought that would allow answering the question, based on the existing measured data, whether the activation energy of plastic deformation depends on temperature. The solution proved to be designing a mathematical model that would describe deformation curves. The original intention was to write one function of all three variables $\sigma=\sigma(\varphi,t,\varphi')$ for 25 measured deformation curves. Although this was achieved, it was not used due to accuracy issues of the calculated deformation resistance values. Therefore, five separate functions $\sigma = \sigma(\varphi, t)|_{\varphi=const}$ were written for each graph in **Fig. 1** (for each deformation rate). Deformation resistance as a function of deformation and deformation temperature at a constant deformation rate value is expressed by Eq. (18). The calculated regression

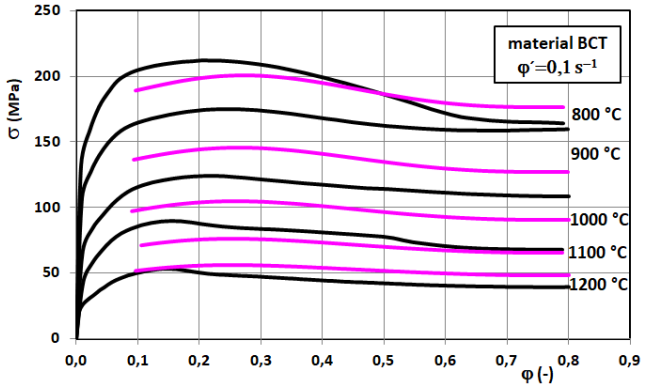

Fig. 5 Measured and calculated values of deformation resistance according to Eq. (19)

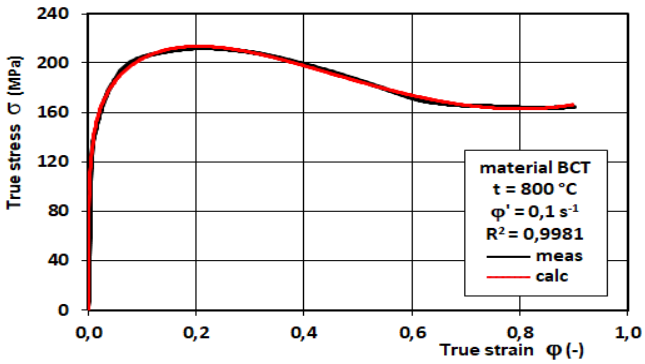

Fig. 6 True Strain –True Stress curve for BCT steel

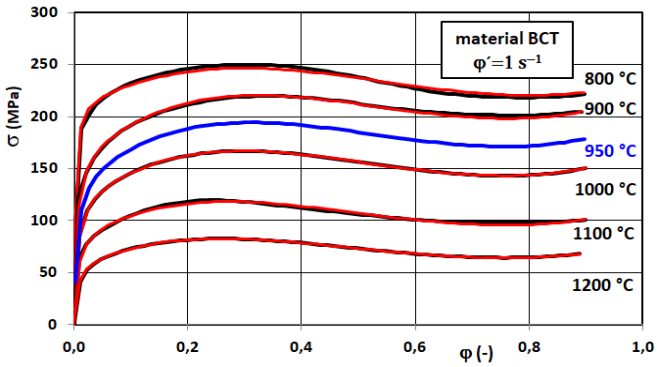

Fig. 7 True Strain –True Stress curves for the rate of deformation φ'=1 s^{-1}

coefficients for individual deformation rates in semi-logarithmic form and the corresponding correlation coefficient R^2 are given in **Table 7**. The physical modeling of refining the deformation temperature step was replaced by numerical modeling based on the mathematical model Eq. (18) with coefficients according to **Table 7**. A clear demonstration of numerical modeling of deformation curves for deformation rates of 0.001, 0.01, 0.1, 1, and 10 s^{-1} in the temperature range

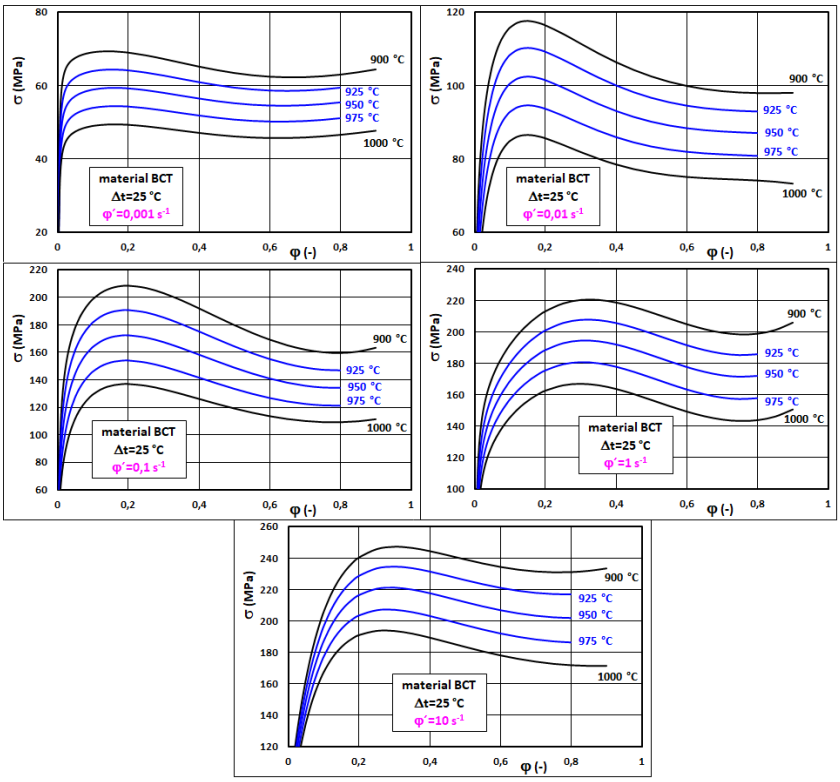

Fig. 8 Measured and calculated True Strain –True Stress curves

Table 7 Regression coefficients for Eq. (15)

Coefficient	Function	φ´=0.001 s^{-1}	φ´=0.01 s^{-1}	φ´=0.1 s^{-1}	φ´=1 s^{-1}	φ´=10 s^{-1}
$ln\ \sigma_0$	1	-1.554 520E+03	1.459 077E+03	-3.753 950E+02	-4.944 155E+03	-8.922 110E+03
a_0	$ln\ \varphi$	-8.089 760E+02	-4.019 672E+02	3.275 665E+03	-1.803 995E+03	-4.565 676E+03
a_1	$t.ln\ \varphi$	3.421 374E+02	1.651 044E+02	-1.429 949E+03	7.785 968E+02	1.992 702E+03
a_2	$t^2.ln\ \varphi$	-4.819 608E+01	-2.260 857E+01	2.078 764E+02	-1.120 063E+02	-2.897 604E+02
a_3	$t^3.ln\ \varphi$	2.261 294E+00	1.033 515E+00	-1.006 274E+01	5.370 835E+00	1.403 953E+01
b_1	φ^{-3}	-2.118 706E-08	4.880 244E-12	6.009 430E-10	-2.814 375E-11	-3.570 895E-07
b_2	φ^{-2}	8.559 629E-05	-1.746 064E-06	-1.817 740E-05	1.263 285E-05	6.724 592E-04
b_3	φ^{-1}	-1.905 108E-02	3.108 290E-02	8.812 151E-02	-2.221 706E-02	-1.661 923E-01
b_4	φ	-6.520 699E+01	-6.544 728E+01	-9.254 156E+01	7.085 591E+00	8.947 487E+00
b_5	φ^2	4.344 192E+01	1.020 775E+02	1.264 784E+02	-4.533 485E+01	-9.222 651E+00
b_6	φ^3	-1.532 985E+01	-5.680 636E+01	-6.274 135E+01	3.528 811E+01	1.526 459E+00
b_7	t	6.447 924E+02	-7.021 541E+02	1.134 173E+02	2.115 369E+03	3.873 630E+03
b_8	t^2	-8.452 027E+01	1.121 100E+02	-8.792 280E+00	-3.008 617E+02	-5.596 058E+02
b_9	t^3	3.626 041E+00	-5.924 085E+00	5.240 818E-02	1.423 772E+01	2.692 039E+01
b_{10}	$t^{-1}.\varphi^3$	1.489 989E-07	–	-4.147 687E-09	–	-4.773 591E-03
b_{11}	$t^{-1}.\varphi^2$	-6.018 040E-04	1.105 036E-05	1.251 116E-04	-8.021 757E-05	1.194 036E+00
b_{12}	$t^{-1}.\varphi^{-1}$	1.206 831E-01	-2.128 650E-01	-6.124 560E-01	1.331 240E-01	-8.154 774E+01
b_{13}	$t^{-1}.\varphi$	5.467 399E+01	4.272 054E+02	6.267 982E+02	-3.826 050E+01	7.470 249E+01
b_{14}	$t^{-1}.\varphi^2$	-1.205 994E+02	-6.788 033E+02	-8.728 506E+02	2.831 714E+02	-1.227 263E+01
b_{15}	$t^{-1}.\varphi^3$	6.971 215E+01	3.814 472E+02	4.379 169E+02	-2.239 982E+02	2.532 149E-06
b_{16}	$exp(-\varphi)$	-5.778 381E+01	–	–	–	–
R^2	–	0.9972	0.9919	0.9959	0.9990	0.9980

t=900 to 1000 °C with a step of Δt=25 °C is shown in **Fig. 8**. Black deformation curves for t=900 and 1000 °C were measured via physical modeling, while blue deformation curves for temperatures t=925, 950, and 975 °C were obtained by numerical modeling. This approach refines the temperature step for deformation for all measured deformation curves shown in **Fig. 1**. In this temperature interval, for deformation from φ=0.10 to φ=0.80 with a step Δφ=0.05, 15 data matrices of deformation resistance were needed. Garofal's Eq. (18) can be applied 15 times to this extended data set. For the temperature range 800 to 900 °C, numerical modeling supplemented the deformation curves for 825, 850, and 875 °C at all 5 deformation rates. In the 900 to 1000 °C range, curves for 925, 950, and 975 °C were added. The temperature interval of 1000 to 1100 °C is supplemented with deformation curves for 1025, 1050, and 1075 °C, and the 1100 to 1200 °C interval with curves for 1125, 1150, and 1175 °C. From the calculated energy values, four curves showing the functional dependence of activation energy on deformation were constructed. Visualization of these curves is shown in **Fig. 9**.

This graph demonstrates the dependence of activation energy on temperature. With increasing deformation temperature, the activation energy also increases. If the temperature step of deformation were further refined and the activation energy recalculated, it would approach the activation energy value for a specific deformation temperature. From previous considerations, it follows that the activation energy of hot plastic deformation is not constant but depends on deformation temperature. Generally, literature [1-23] states that activation energy for hot plastic deformation over the entire temperature range of forming is constant. The temperature step of deformation curves was refined by numerical simulation to Δt=6.25 °C. An example visualization of such a mathematical simulation for compression conditions t=1000 to 1025 °C and deformation rate $\dot{\varphi}$=1 s^{-1} is shown in **Fig. 10**. The black curve marked as *Meas* represents the deformation curve obtained from physical simulation. The blue curve represents the deformation curve obtained in the first step of the numerical simulation, labeled *CalcI*, and the three purple deformation curves were obtained in the second step of the numerical simulation, labeled *CalcII*.

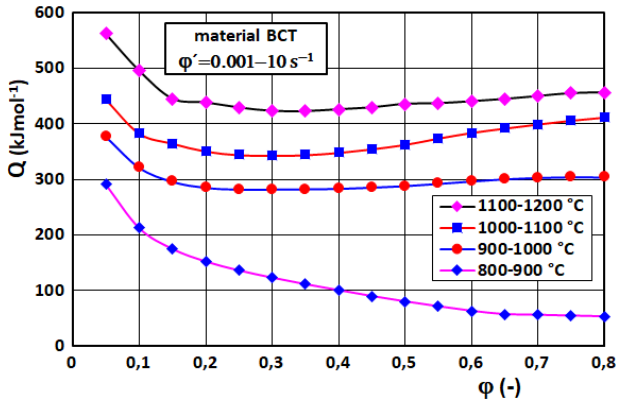

Fig. 9 Dependence of activation energy on deformation

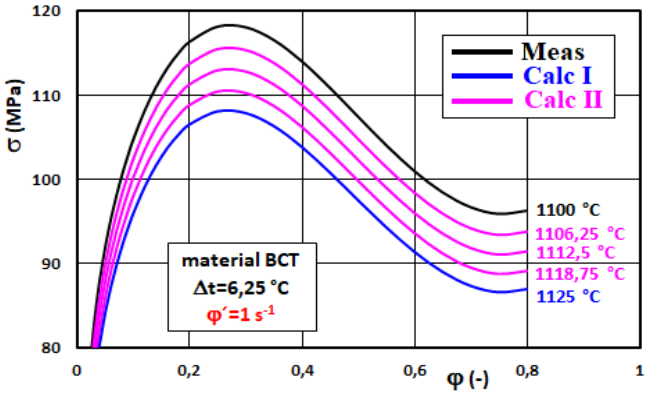

Fig. 10 Physical and numerical simulation

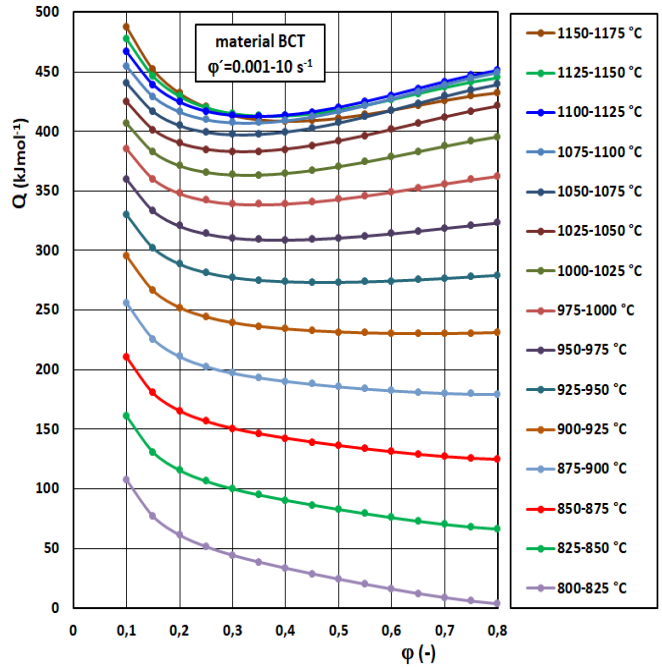

Fig. 11 Dependence of activation energy on deformation

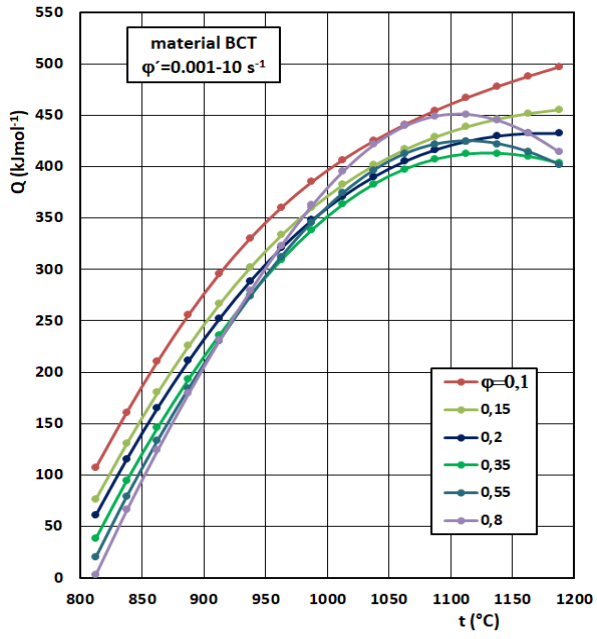

Fig. 12 Dependence of activation energy on temperature

A total of 240 activation energy values were calculated for the entire compression test experiment. The visualization of activation energy versus deformation is shown in **Fig. 11**. Each curve corresponds to a different temperature range, with a step value of Δt=25 °C. The temperature range is assigned a representative point value corresponding to its midpoint. For example, the temperature range 800 to 825 °C is assigned to the point value 812.5 °C, the range 825 to 850 °C is assigned 837.5 °C, and so forth. Each point temperature value is associated with its corresponding activation energy value. The resulting visualization of activation energy as a function of temperature is shown on **Fig. 12**. The graph reveals that as temperature increases, activation energy also rises. The set of curves in **Fig. 12** has been replaced by a single curve shown in **Fig. 13**. This curve represents the functional dependence of the activation energy *Q(t)* of hot plastic deformation, which can be generally expressed by the mathematical equation:

$$Q(t) = q_0 + q_1 t + q_2 t^2 \qquad (20)$$

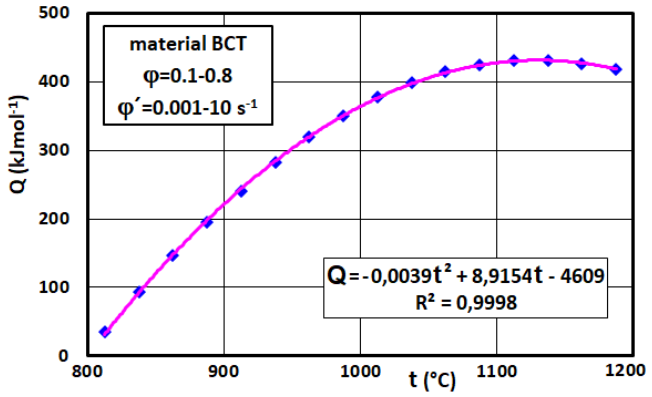

Fig. 13 Dependence of activation energy on temperature

The variable *t* represents the forming temperature given in °C, and the constants q_0, q_1, q_2 have chosen units such that they compensate for the units of the equation to yield the activation energy dimension in kJ·mol^{-1}. The specific values of the constants *q* for BCT steel, valid in the forming temperature range 800 to 1200 °C, are shown in the graph in **Fig. 13**. Furthermore, this applies for deformation in the range φ=0.1 to 0.8 and deformation rate in the range φ'=0.001 to 10 s^{-1}. The mathematical equation of the activation energy shown in **Fig. 13** has a correlation coefficient R^2=0.9998, which demonstrates a direct functional dependence. The graph in **Fig. 13** confirms that the stated hypothesis, that the activation energy of hot plastic deformation is not constant but functionally dependent on the forming temperature, is valid.

CONCLUSIONS

- It was use of a new methodology for calculating the material constants of the Garofalo equation enabled obtaining refined values of the constants
- A specific mathematical model of the hot deformation process for BCT steel was obtained
- The mathematical model allowed numerical simulation of the deformation process during the compression test
- Narrowing the temperature interval of deformation enabled the calculation of activation energy for a narrower range of deformation temperatures
- For BCT steel, the temperature dependence of the activation energy of plastic deformation was established

Acknowledgement: Funded by the EU Next Generation EU through the Recovery and Resilience Plan for Slovakia under the project No. 09I03-03-V04-00694.

REFERENCES

[1] F. Garofalo: Transactions of the Metallurgical Society of AIME, 227, 1963, 351-355.
[2] C.M. Sellars, W.J. McTegart: International Metallurgical Review, 17, 1972, 1-24, https://doi.org/10.1179/imtlr.1972.17.1.1
[3] S.H. Talbert, B. Avitzur: *Elementary Mechanics of Plastic Flow in Metal Forming*. John Wiley & Sons, New York, 1996.
[4] S. Spigarelli, M. Cabibbo, E. Evangelista, J. Bidulská: Journal of Materials Science, 38, 2003, 81-88, https://doi.org/10.1023/A:1021161715742
[5] E.M. Mielnik: *Metalworking Science and Engineering*, McGraw-Hill, New York, NY, 1991.
[6] J. Bidulská, I, Pokorný, T. Kvačkaj, R. Bidulský, M. Actis Grande: High Temperature Materials and Processes, 28(5), 2009, 315–321, https://doi.org/10.1515/HTMP.2009.28.5.315
[7] F. Drastík, J. Elfmark et al: *Plastometers and formability of metals*. Praha, SNTL, 1977, 392 p. (in Czech).
[8] T. Kvačkaj, I. Pokorný: Metalurgija, 34(4), 1995, 145–150.
[9] F. Garofalo: *Fundamentals of Creep and Creep-Rupture in Metals*. The Macmillan Company, New York, 1965.
[10] R. Pernis: Acta Metallurgica Slovaca, 23(4), 2017, 319-329, https://doi.org/10.12776/ams.v23i4.1017
[11] M. El Mehtedi, S. Spigarelli: Acta Physica Polonica A, 128(4), 2015, 722-725, https://doi.org/10.12693/APhysPolA.128.722
[12] R. Pernis, J. Kasala, J. Bořuta: Kovove Materialy-Metallic Materials, 48(1), 2010, 41–46, https://doi.org/10.4149/km_2010_1_41
[13] G. Quan, J. Pan, X. Wang: Applied Science, 6, 2016, 66, https://doi.org/10.3390/app6030066
[14] G. Wei, X. Peng, A. Hadadzadeh, Y. Mahmoodkhani, W. Xie, Y. Yang, M.A. Wells: Mechanics of Materials, 89, 2015, 241–253, https://doi.org/10.1016/j.mechmat.2015.05.006
[15] F. Yin, L. Hua, H. Mao, X. Han: Materials and Design, 43, 2013, 393–40, https://doi.org/10.1016/j.matdes.2012.07.009
[16] L. Li, L. Wang: High Temperature Materials and Processes, 37(5), 2018, 411-424, https://doi.org/10.1515/htmp-2016-0234
[17] G. Quan, C. Yu, Y. Liu, Y. Xia: The Scientific World Journal, 2014, 2014, 108492, https://doi.org/10.1155/2014/108492
[18] R. Pernis, M. Škrobian: Hutnické listy – Metallurgical Journal, 74(1-2), 2021, 11-17 (in Slovak).
[19] J. Bidulska, R. Bidulsky, L. Ceniga, T. Kvackaj, M. Cabibbo, E. Evangelista: Kovove Materialy-Metallic Materials, 46(3), 2008, 151-155.
[20] R. Bidulsky, et al.: Acta Metallurgica Slovaca, 31(1), 2025, 53-58, https://doi.org/10.36547/ams.31.1.2160
[21] T. Kvackaj, J. Bidulská, R. Bidulský: Materials, 14(8), 2021, 1988, https://doi.org/10.3390/ma14081988
[22] J. Bidulská, T. Kvačkaj, R. Bidulsky, M. Grande: High Temperature Materials and Processes, 27(3), 2008, 203-207. https://doi.org/10.1515/HTMP.2008.27.3.203
[23] J. Bidulská, T. Kvačkaj, R. Bidulsky, M. Grande: Kovove Materialy-Metallic Materials, 46(6), 2008, 339-344.